CFD Modelling and Simulations of the HYPROB Regenerative LOX/CH4 Thrust Chamber

Pietro Roncioni, Daniele Cardillo, Mario Panelli, Daniele Ricci, Marco Di Clemente, Francesco Battista
CIRA (Italian Aerospace Research Centre)
Via Maiorise, 81043 Capua (CE), Italy

Abstract
The work described in this paper has been conducted in the framework of the HYPROB Program that is carried out by the Italian Aerospace Research Centre (CIRA), under contract by the Italian Ministry of Research. The Program has the main objective to enable and improve National System and Technology capabilities on liquid rocket engines (LRE) for future space propulsion systems and applications, with specific regard to LOX/LCH4 technology. In this paper all the CFD simulations aimed at investigations of the combustion phenomena inside the thrust chamber, including the regenerative cooling of supercritical methane, are reported and discussed.

1. Introduction

The HYPROB Program is carried out by CIRA, the Italian Aerospace Research Centre, under contract by the Italian Ministry of Research. The Program has the main objective to enable and improve National System and Technology capabilities on liquid rocket engines (LRE) for future space propulsion systems and applications, with specific regard to LOX/LCH4 technology. The Program is structured in 3 main development lines, each corresponding to a specific implementation project: System: design and development of technology LRE demonstrators, including intermediate breadboards; Technology: R&T development in the areas of CFD combustion modelling, thermo-mechanical modelling and materials, advanced optical diagnostics; Experimental: testing capabilities for both basic physics and system-oriented (demonstrators) experimentation.
The first implementation of the Program (the system line), named HYPROB BREAD, has been launched; it is aimed at designing, manufacturing and testing a LRE demonstrator, of three tons thrust, based on a regenerative cooling system using liquid methane as refrigerant. The HYPROB-BREAD project foresees, in the development of the complete system, the design of various breadboards aimed at the investigation of critical design aspects such as the supercritical behaviour of the methane and the mixing and combustion processes of the propellants (gaseous methane and liquid oxygen). The above-said breadboards are described in [1].
The HYPROB-BREAD Project design activities have been conducted during the preliminary phase mainly by means of engineering methods (ECOSIMPRO, etc.). However, a cross check with CFD numerical simulations was needed in order to be confident with the results of the design activities. Moreover, an extensive use of CFD codes has been necessary not only for the cross checks with the engineering tools but also as an advanced design tool.

2. System Description

The final aim of the program is the building of a LOX/CH4 liquid rocket engine demonstrator whose high-level requirements can be summarized as follows: thrust class of 30 kN; relevant to future applications of space propulsion; pressure-fed testing; regenerative cooling with liquid methane; ability to reproduce an expander cycle engine. Several steps are foreseen in order to obtain this technological target and in particular the building of intermediate breadboards which can enable the analysis and validation of the most critical design solutions as the design of the combustion chamber and its injection plate as well as the regenerative cooling. The use of existing know-how and design solutions for the above-said critical items is the baseline, nonetheless the development of new design strategies taking particularly into account the methods of the computational fluid-dynamics are strongly emphasized during all over the program.

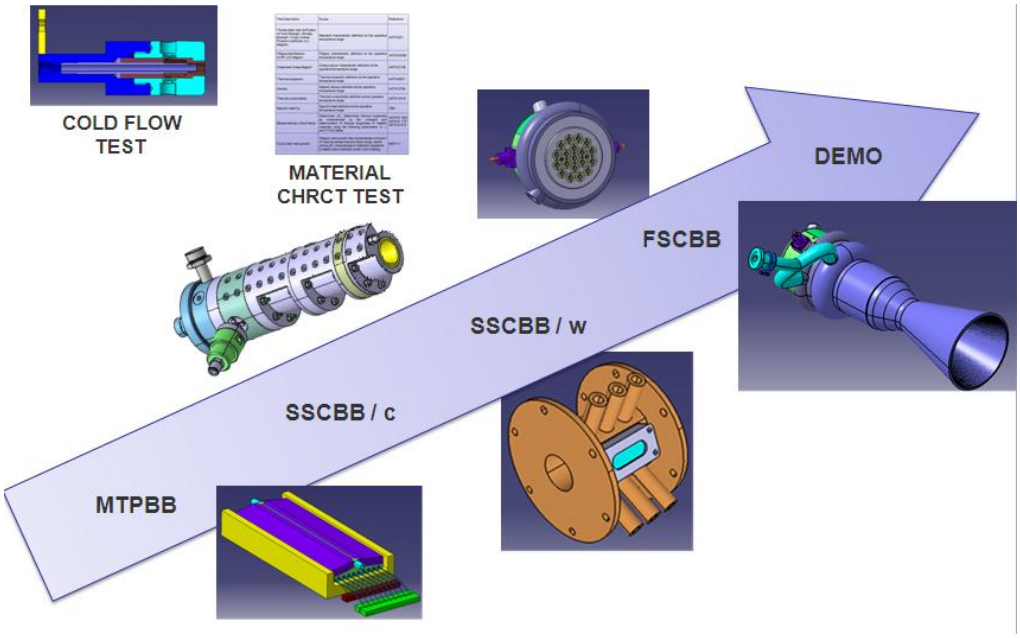

Figure 1: Logical steps of LOX/CH4 Demonstrator development.

Following the above reported logical steps (Figure 1), four products shall be produced in the frame of the project, namely three technological breadboards and one demonstrator:
• The first breadboard is designed in order to investigate methane thermal behaviour in heating processes (MTP breadboard);
• The second breadboard (SSBB) aim is to investigate combustion and heat transfer phenomena into two subscale modular calorimetric thrust chambers: the basic calorimetric sub-scale breadboard (SSCBB/c) is focused on the investigation of heat transfer to chamber wall, while the second one (SSCBB/w), provided with a windowed optical access, on mixing and combustion processes;
• A third breadboard is foreseen, namely Full Scale Calorimetric Breadboard (FSBB or FSCBB), water cooled, whose aim is to allow the demo injection head qualification;
• Finally the demonstrator, that is a regenerative cooled chamber LOX/LCH4 of 30-kN-class of thrust.

2. Results

In this section the numerical results concerning the combustion phenomena (SSBB, DEMO) and the regenerative cooling process (DEMO) are reported. The results of the MTP Bread Board are not reported here since they are subject of other works; moreover, the numerical approach followed is similar to what done for the Demonstrator Cooling Channels.
All the numerical results are the output of a massive use of "quick" CFD simulations mainly oriented to give phenomenological trends in a reasonable CPU convergence time. Deep analyses (characterized by grid convergence and mathematical modelling and numerical schemes sensitivity analyses) have been also conducted but only on a reduced number of tests. At the time of writing this paper, experimental data are not yet available and so a full Verification and Validation procedure (V&V) is not possible for the CFD numerical tools. These quick CFD analyses, conducted following engineering criteria (or requirements), and used in concurrence with engineering tools (ECOSIMPRO, etc.) can be used in the design processes and, from this point of view, give thermal and mechanical input for the structural analyses. The commercial code Fluent v13 has been used for the most part of the simulations ([5], [6]).
The simulations concerning the SSBB have the main aim to study the basic combustion phenomenon and to find the most effective numerical strategy to apply for the subsequent support to the design activities of both the SSBB itself and the FSBB and DEMO products.
The combustion process inside the Demonstrator chamber and the regenerative cooling inside the channels are strongly coupled, anyway at this moment a whole simulation is not affordable and so weak coupling is being done: the Heat Flux on the combustor and nozzle walls, obtained with combustion process simulation, is used as input for the simulation of one of the cooling channels in order to have the thermodynamic characteristics of methane at the exit. The resulting wall temperature is used as new boundary condition for combustion process simulation.

2.1 SSBB

Several numerical simulations have been conducted on the Sub Scale Bread Board (SSBB, see Figure 2) in order to understand the basic mixing and combustion phenomena. The SSBB is a scaled version of the three tons thrust LRE Demonstrator with only one injector (co-axial with tip recess) and represents an intermediate step of the project from an experimental and a numerical point of view (validation of CFD codes). Both axisymmetric and full 3D simulations have been conducted aimed mainly at the evaluation of the wall heat fluxes. However, other important quantities, as the chamber pressure, have been verified.

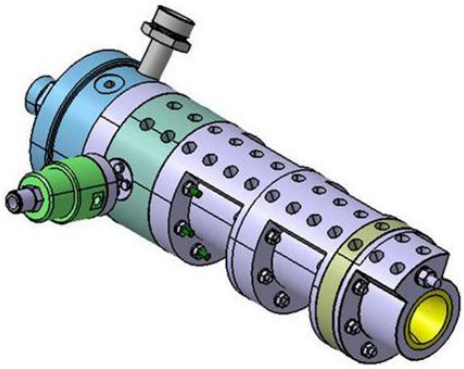

Figure 2: Sub Scale Bread Board 3D view (left) and section (right).

The first computations were made on a partial 2D configuration, where nozzle has been omitted in order to make the simulation simpler and quicker, with the aim to evaluate the injector characteristics. The computations on the 2D full configuration were performed with the aim to evaluate the equilibrium chamber pressure and the combustion efficiency, as well as heat flux on the nozzle walls. Figure 3 shows the 2D domain with the related boundary conditions. Both LOX than CH_4 injector walls and tip have been considered adiabatic, while an isothermal wall at 300K has been imposed for plate, chamber and nozzle. Inlet conditions for the propellants are reported in Table 1.

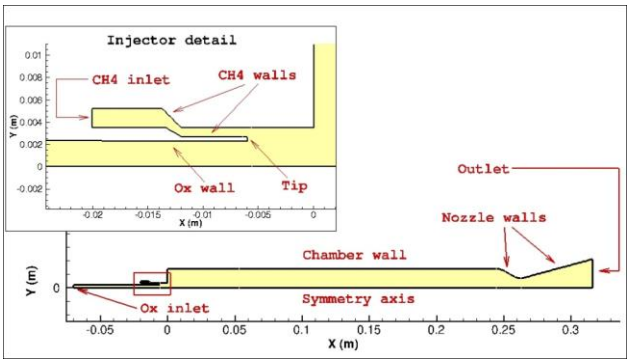

Figure 3: Boundary Conditions on the 2D domain.

Table 1: Boundary Conditions

		mdot [kg/s]	**p [bar]**	**T [K]**
LOX	inlet	0.363084	55	110
GCH4	inlet	0.106789	55	300
	outlet	/	1	300

All the meshes, used for the computations, have been created by means of ANSYS *ICEMCFD*. Two-dimensional computations have been performed both on Low-Reynolds approach, by means of Enhanced Wall Treatment (EWT), and on grid without stretching at wall, while 3D computations have been performed only by means of the latter, using Standard Wall Functions (SWF). All the grids are characterized by cells clustering in the mixing region and in

the first part of the chamber, along the axial direction. The ratio between adjacent cells is everywhere less than 20%. The mesh quality is assured by means of the verification of the determinant, higher than 0.6 for the most critical 3D geometry. Table 2 reports some characteristics of the computational grids.

Table 2: Computational meshes characteristics

	Number of blocks	**Number of cells**	**Height of the first cell at wall [m]**
2D SWF	15	18330	1e-4
2D EWT	15	36932	5e-7
3D	96	714576	1e-4

A pressure-based approach has been adopted for the solution of Navier-Stokes equations in turbulent conditions with a not-segregated algorithm, specifically COUPLED, which allows for the pseudo-transient option. Because of the operating values of pressures and temperatures the oxygen jet is supercritical, therefore the hypothesis of ideal gas could led to overestimation in temperatures (because of the differences in the Cp values close to the critical temperature) with consequences on viscosity, then on Reynolds number, affecting mixing and consequently the jets potential core lengths. Therefore, the use of real gas equation of state, specifically Peng-Robinson, has been necessary. Turbulence has been modelled implementing the standard k-ε with both standard wall functions and enhanced wall treatment, depending on the mesh. Kinetic schemes have been chosen ranging from the simplest 1-step Westbrook-Dryer [9] to the 4-steps Jones-Lindstedt [10], that permits to limit the number of reactions and species but taking into account also the intermediate species in the flame. To take into account chemistry-turbulence interaction, the *Eddy-Dissipation Concept* (EDC) approach has been used; it allows to incorporate detailed Arrhenius chemical kinetics in turbulent flames. On the other hand, also the EDM Eddy Dissipation Model (in this case multi-step kinetic schemes cannot be adopted) and the LFR Laminar Finite Rate have been implemented ([5]).

One of the critical point of these simulations is the severe density gradient due to the supercritical oxygen jet. As it expands into the gas, the oxygen flow diverges away from the LOX core, creating a recirculating region. It is very important to evaluate the size of the recirculation zone past the injector and the position of the stagnation point since they could greatly affect the wall heat flux distribution. An equally important role may be expected to be played by the recirculation zone in the flame anchoring mechanism. Figure 4 displays temperature field with velocity stream-traces for the reactive axi-symmetric simulation using the modeling reported in Table 3. Specifically, recirculating region is highlighted together with the predicted stagnation point. Flame is anchored to the oxygen post-tip.

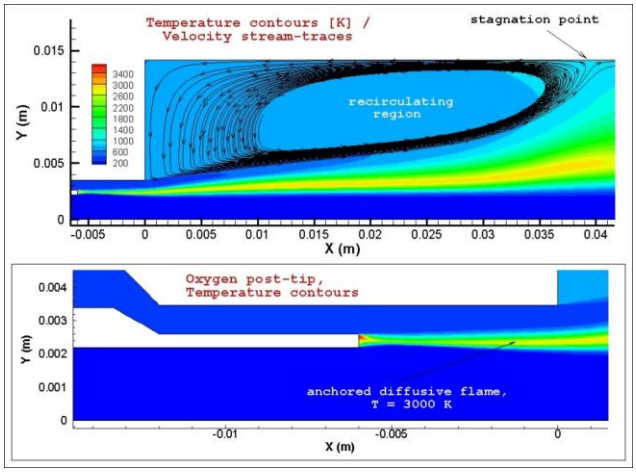

Figure 4: Temperature contours and velocity stream-traces for an axi-symmetric 2D computation.

The thermal field of Figure 4 shows that temperature reaches about 3500 K, even if a mono-step kinetic scheme has been adopted because of the implementation of the EDM combustion model, therefore higher values should be expected. The reason why these temperature values have been obtained is due to the imposition of an artificial methane formation enthalpy, whose value has been modified in order to lower the adiabatic flame temperature to realistic values, of the order magnitude of those predicted by the Jones-Lindstedt more accurate kinetic scheme

(implemented by means of Arrhenius equation). This artifice allows the use of EDM without overestimations in temperature that may bring to overestimations in heat flux values.

Table 3: Modelling adopted for the results showed in Figure 4.

Grid	2D SWF partial conf.
Equation of State	Peng-Robinson
Turbulence Model	k-ε
Turbulent Comb. Model	EDM
Kinetic Scheme	Mono-step

The implementation of different combustion models, i.e. EDM and EDC, led to completely different results. Figure 5 shows the temperature contours in the computational domain for both the simulations, highlighting the mixing region, from which it is possible to deduce that in the EDM prediction the flame is anchored to the oxygen post-tip while in the EDC case it is not anchored in this point. The nature of the flame changes as a function of the turbulence-chemistry interaction model under examination. Figure 6 and Figure 7 show the contours of alpha for the EDC and the EDM simulation, respectively, that represents the angle between fuel and oxidizer concentration gradients. If such gradients are opposed the flame is diffusive in nature (values in the images greater than $\pi/2=1.57$) otherwise, if aligned, the flame tends to acquire a pre-mixed character. Figure 6 shows that values are lower than $\pi/2$ where the flame is predicted by using the EDC model (pre-mixed flame), while Figure 7 shows that they are higher than $\pi/2$ where the flame is predicted by the EDM model (diffusive nature of the flame).

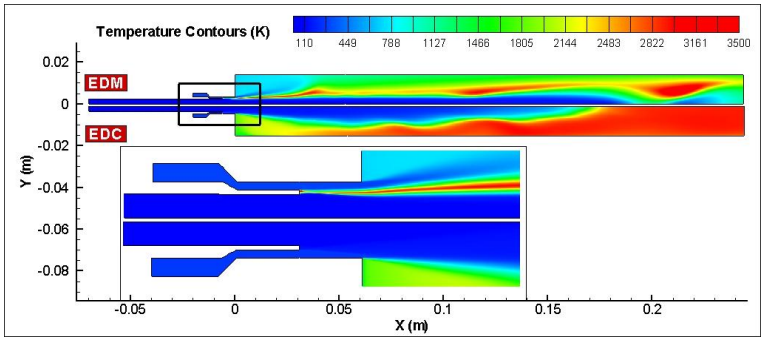

Figure 5: Comparison in terms of temperature fields for EDM and EDC numerical predictions

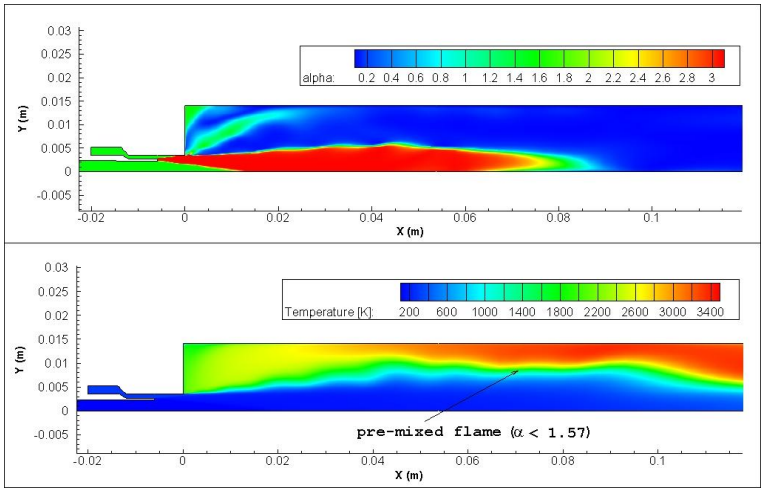

Figure 6: Contours of alpha (top) and temperature (bottom) for the EDC simulation.

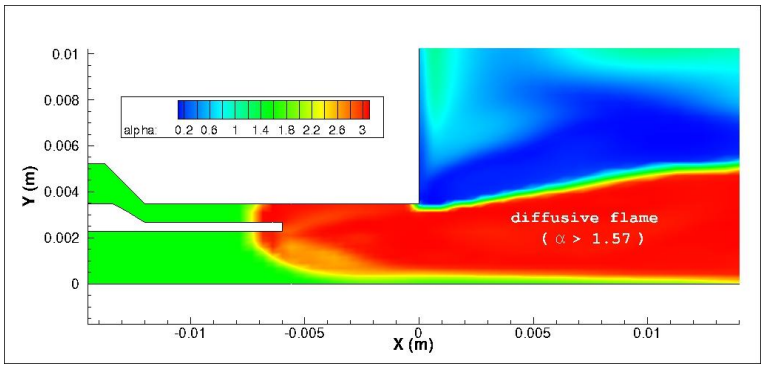

Figure 7: Contours of alpha for the EDM simulation

This situation does not allow to be confident about the flame anchoring mechanism. It seems that flame is anchored to the tip for the EDM model, but not for the EDC model. Another computation, performed implementing the Laminar Finite Rate combustion model together with the Jones-Lindstedt kinetic scheme (which predicts with good accuracy the time ignition delay, responsible of the anchoring mechanism), has predicted a diffusive flame anchored to the oxygen post-tip (see Figure 8). Therefore we are led to believe that EDC prediction is less realistic than that associated to the use of other combustion models, and that a diffusive flame should come from. Moreover the recirculating phenomenon could help the mechanism of anchoring leading to a situation where flame is detached from the tip and anchored a little farther from the injector. However, the diffusive nature of the flame should dominate the phenomenon under examination leading to a type of flame similar to those predicted by EDM or LFR.
In Figure 8 the predicted fields of pressure, temperature, and H2O mass-fraction are displayed on the full 2D configuration, comparing the results predicted by using both EDM with mono-step kinetic scheme and LFR with Jones-Lindstedt mechanism. The equation of state and the turbulence model are those reported in Table 3. Although a statistical convergence is reached, local fluctuations of the RANS field were not eliminated; this could be due to acoustic properties of the chamber (presence of unsteady wave phenomena and their interaction with the reacting field) or to numerical causes. The average pressure values are 51.64 and 53.04 bar for, respectively, EDM and LFR simulations. Other computations, changing grid refinement and test modeling, showed a range of predicted average pressure between 49 and 53 bar. These values, lower than the nominal one, determined by the use of engineering tools, lead to think that combustion efficiency could be overestimated by the tools, leading, the latters, to an optimistic situation characterized by higher values of chamber pressure.

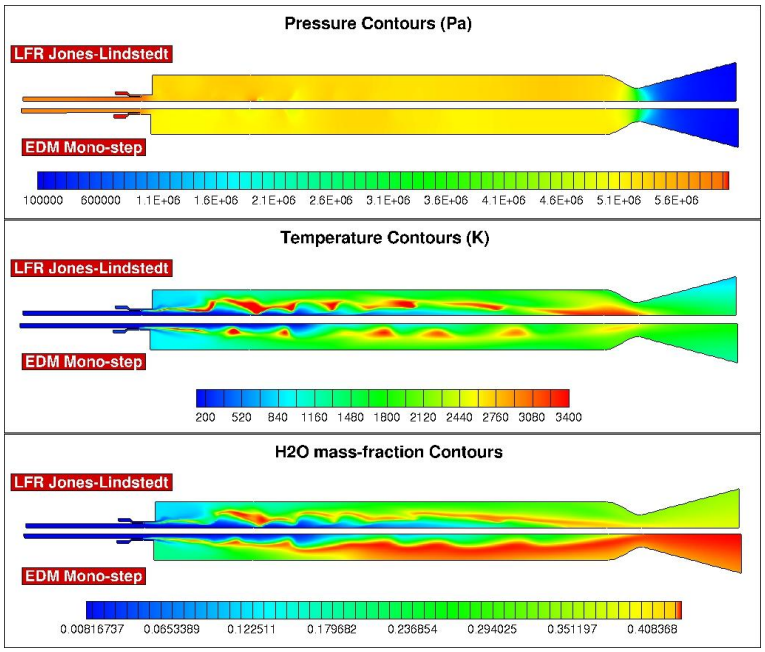

Figure 8: Pressure, temperature and H2O mass-fraction contours for EDM and LFR combustion models.

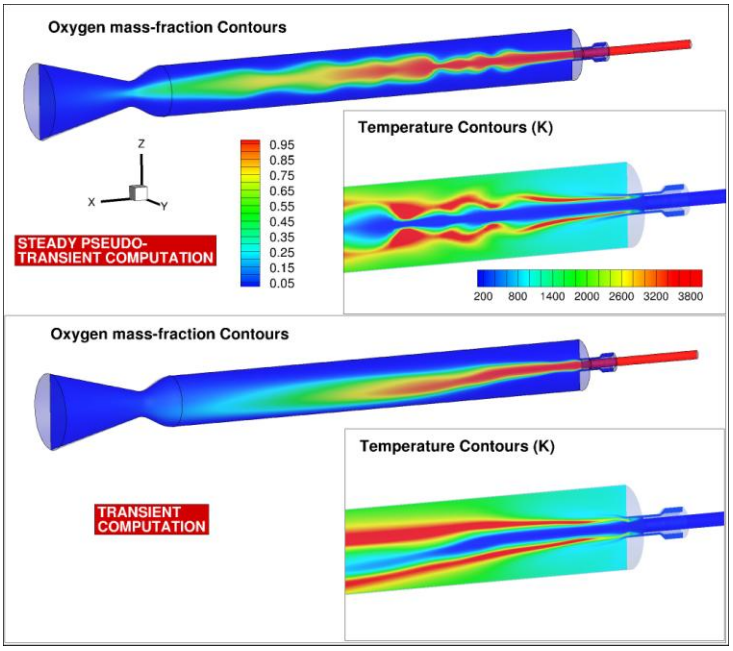

Figure 9: Temperature distributions on different planes for the 3D results.

The 3D results have been performed only by implementing the EDM combustion model using SWF. In this case both steady "pseudo-transient" and transient computations have been performed. The results show that the pseudo-transient simulation confirms the prediction of the axi-symmetric computations: the recirculating region is nearly the same, as well as chamber average pressure and distributions of temperature and heat fluxes. Moreover, the solution is symmetric with respect to the X-axis (see Figure 9, where temperature contours are showed on the plane Y=0). On the contrary, the solution predicted by the transient simulation is characterized by asymmetries even if the average values are nearly the same. Furthermore it is worth to notice that the fluctuations observed in the steady computations disappeared in the transient simulations. Therefore they should be related to numerical reasons.
Figure 10 shows the heat flux distribution along the chamber wall; it is worth to underline that a grid without stretching at wall has been used, paying attention to the Y+ value, ranging in the limit of the correct use of Standard Wall Functions ($30 < Y+ < 300$). In particular, the results obtained by using EDM, LFR with a simplified mono-step scheme and LFR with a more detailed Jones-Lindstedt mechanism are compared. In the case of EDM the lowest heat flux values are predicted (except in the nozzle throat), with a peak in proximity of the stagnation point downstream of the recirculating zone of about 10 MW/m2, versus 12 MW/m2 of the LFR mono-step and 14 of the LFR Jones-Lindstedt. Along the chamber wall LFR mono-step and Jones-Lindstedt are in good agreement, while EDM deviates significantly from the latter. Little lower heat flux values have been observed by using a low-Re grid with EWT.

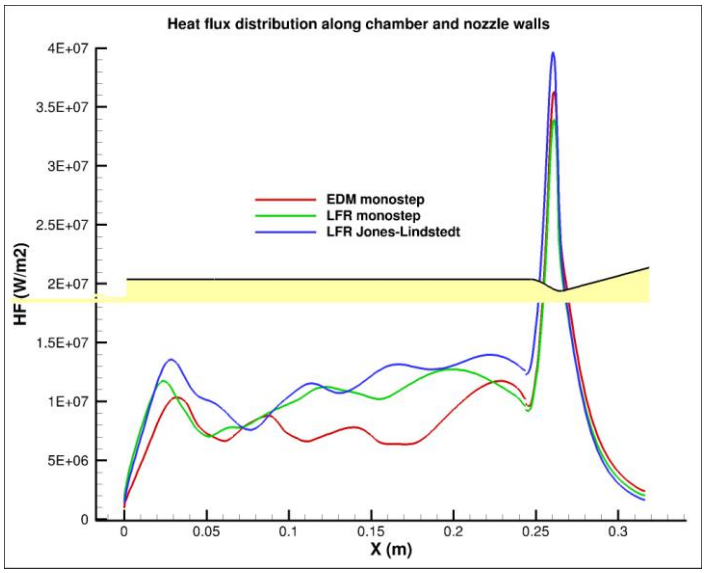

Figure 10: HF distributions along the chamber and nozzle walls predicted by the using of different models.

2.2 DEMONSTRATOR

The analysis of the thrust chamber (the Demonstrator, Figure 11, left) is aimed, as in the case of previous Bread Board, at the estimation of the thermal and mechanical loads necessary for the structural design and at the characterization of the propellant mixing and combustion and flame structure evolution.

The simulations have been performed both with the hypothesis of an axisymmetric flow and in 3D configuration (Figure 11, right). The injectors' dimensions of the 2D model were scaled in order to fix both the mass flow rate and the momentum flux of the real demonstrator. Figure 12 shows the comparison of the H_2O field, used to identify the flame shape.

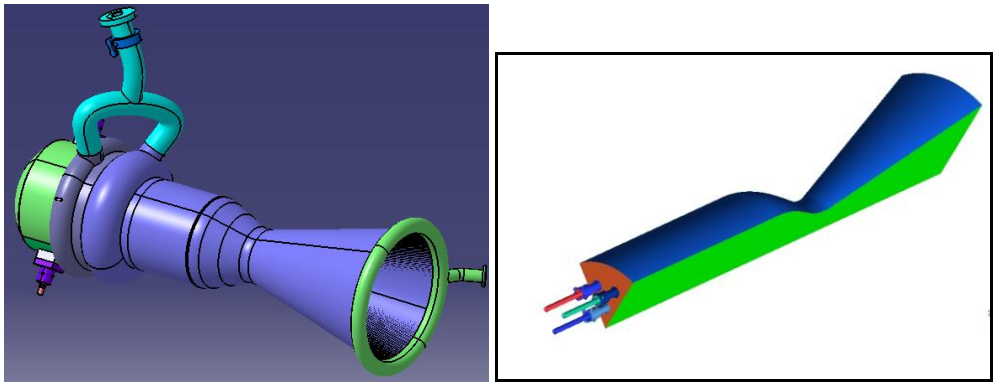

Figure 11: LRE Demonstrator (left); 60° wedge for 3D simulations (right).

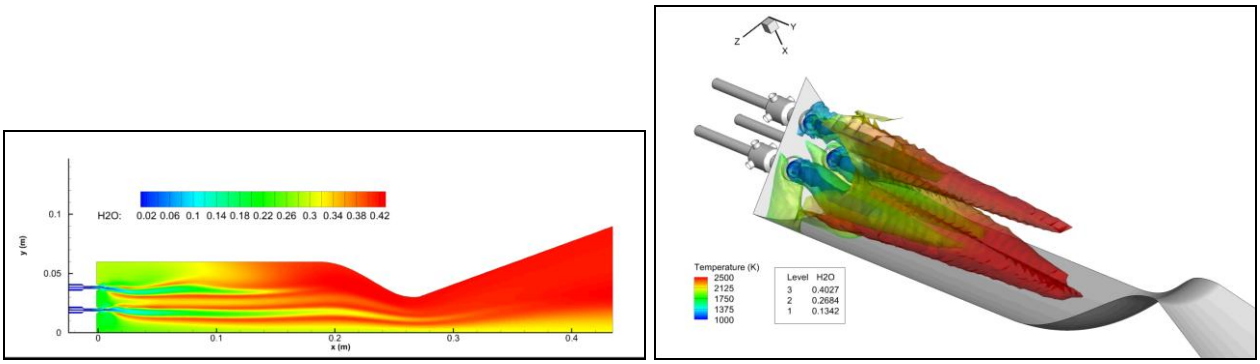

Figure 12: Demo: 2D Axisymmetric contour plot compared to 3D isosurface of H2O.

The results showed a good comparison confirming that the use of simplified configurations (axisymmetric) can be used during the first steps of the design (Figure 13): particularly the heat flux throat peak intensity did not change deeply using a 3D model. The main difference was the heat flux peak on the combustion chamber, 2cm far from the injection plate, which affected deeply the shape of the cooling channel and led preferred the choice of a 3D model in the detailed design review.

The heat flux on the injection plate was very sensible to the flame shape, consequently an axisymmetric model had only been used to predict average values on it but not local one (Figure 14). Only with 3D simulations it had been possible to calculate more reliable surface heat flux distributions. A grid sensitivity analysis was performed on the local cells' distribution in the mixing layer between fuel and oxidant. The results (Figure 15) show that the flames moved away from the injection plate and, consequently, both the average and the peak heat fluxes decreased in intensity. The three heat flux peaks in the middle of the plate and between the ring of injectors, foreseen by the coarse level of grid n.1, disappeared when the grid became fine in the mixing region (grid n.2, 3). The two remaining peaks were localized between the external ring injector and the combustion chamber, where the hot gases were carried back to the plate from the local recirculating region. The data of average and peak heat fluxes on the injection plate are plotted in Figure 16 (right).

The changes of the flame position affected also the peaks of heat flux on the combustion chamber (Figure 16, left) that moves forward and seemed to stabilized 3cm far away from the plate.

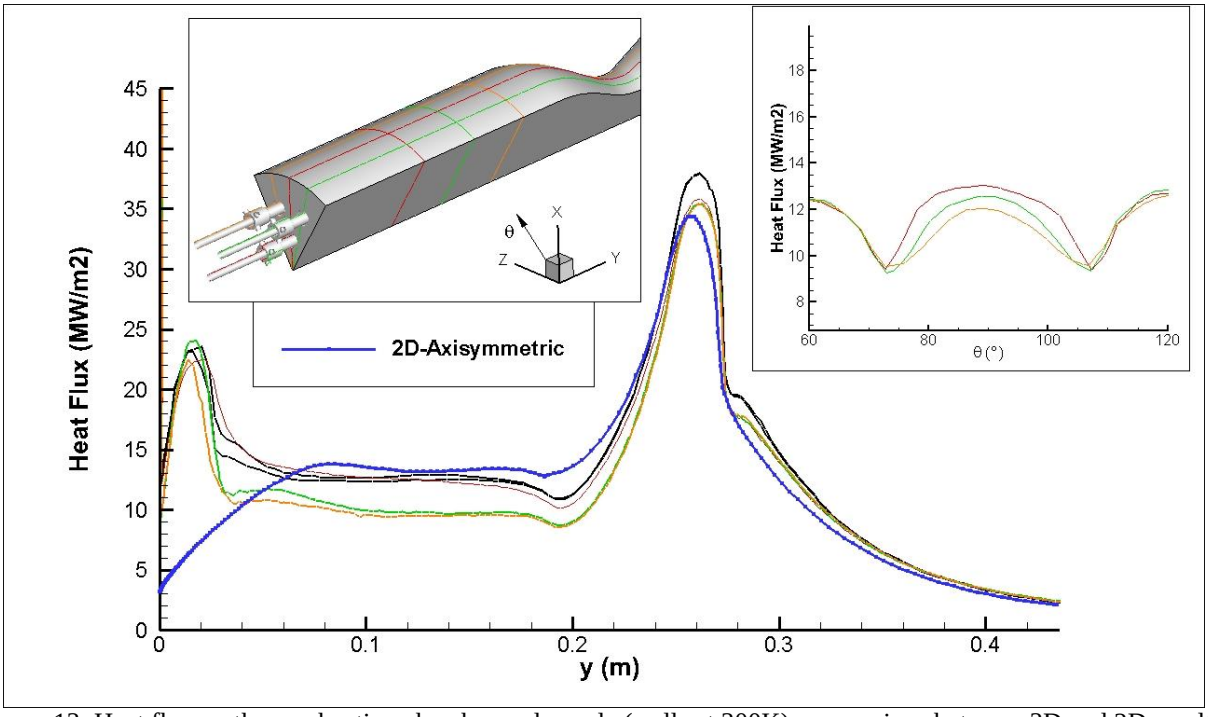

Figure 13: Heat flux on the combustion chamber and nozzle (walls at 300K); comparison between 3D and 2D results.

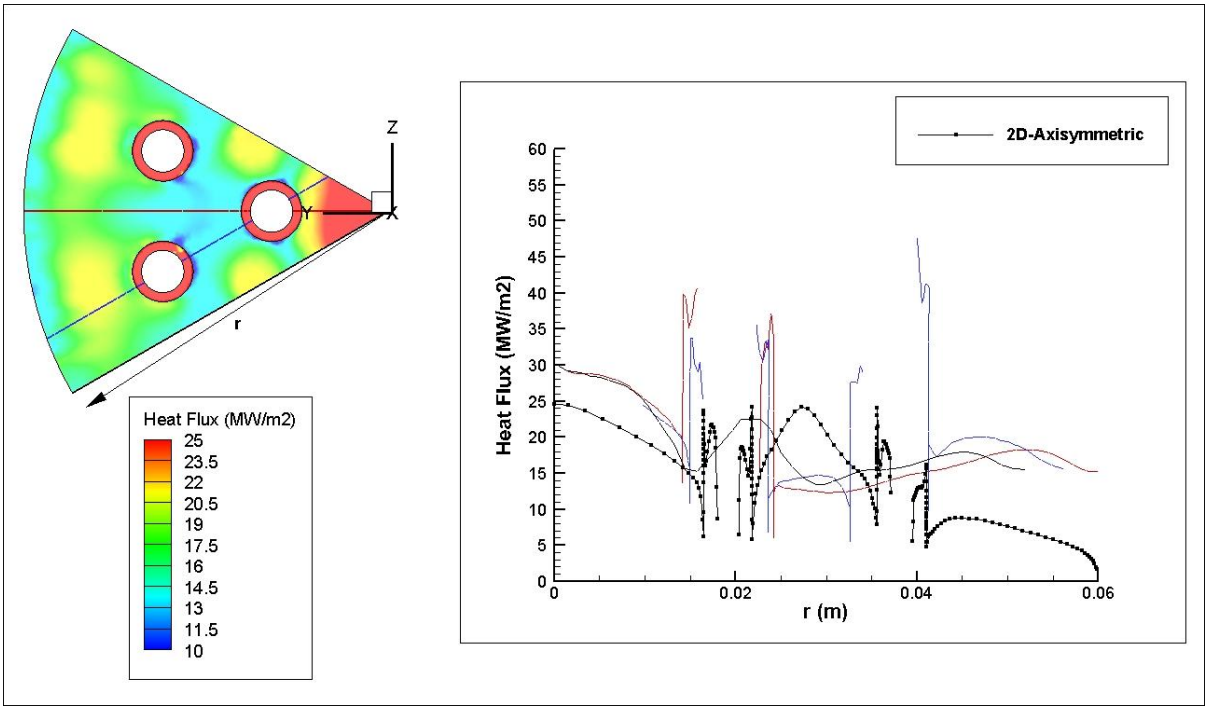

Figure 14: Heat flux on the injection plate (isothermal at 300K); comparison between 3D and 2D results. The peaks on the injectors' ring are not reliable.

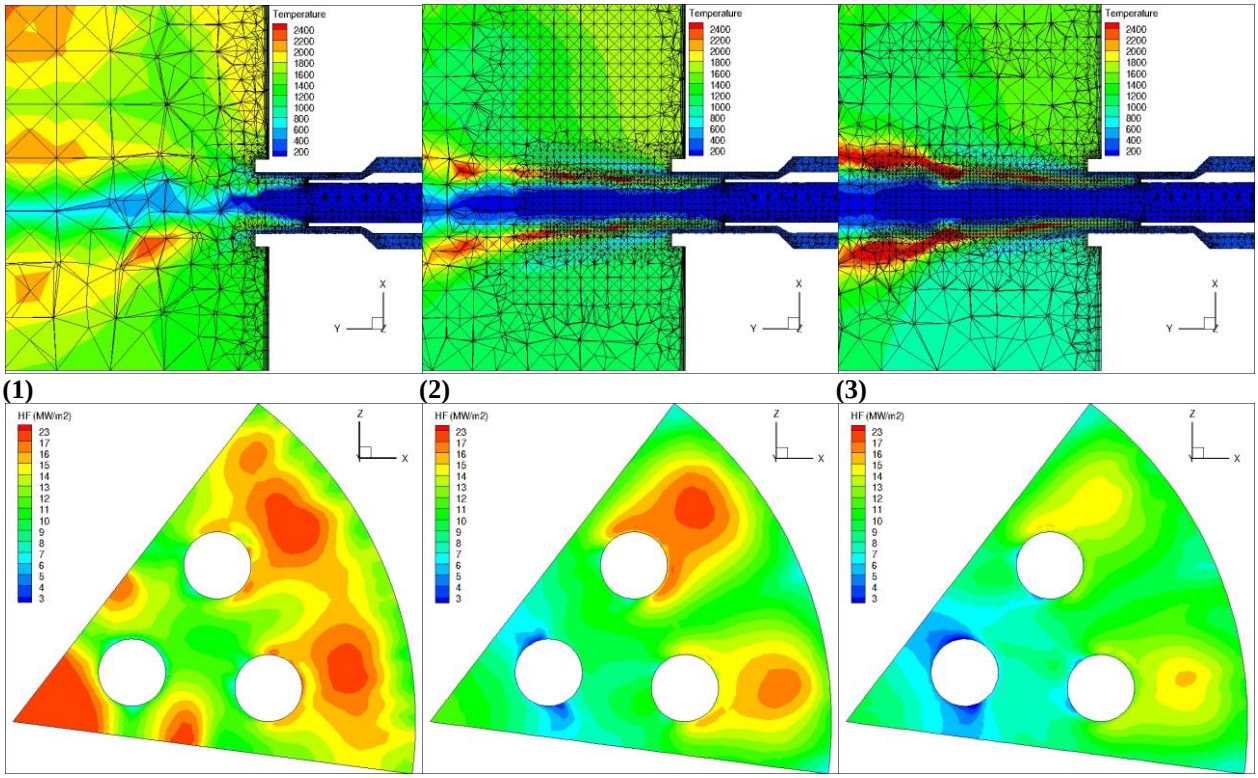

Figure 15: Heat Flux (HF) on the injection plate (isothermal at 550K); meshes and temperature (K) contour plots.

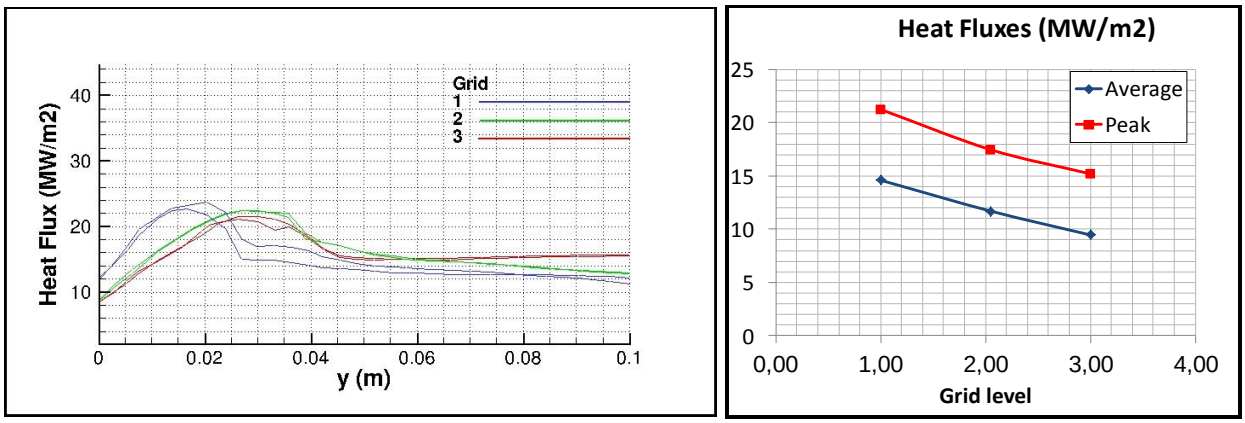

Figure 16: (left) Displacement of the heat flux peak on the combustion chamber near the injection plate. Note: the two lines per grid are taken from the side of the wedge domain. (Right) Grid level sensitivity.

2.3 DEMONSTRATOR Cooling Channel

One of the most important aspects of the project is the study of the regenerative cooling jacket, fed by the fuel (methane) and, in particular, the coupling between the external cooling counter flow and the internal hot combustion products flowing from the injectors to the nozzle. The cooling jacket has been designed by means of an iterative procedure, adopting a 1-D approach with 2-D corrections and interpolating the fluid properties of methane by NIST tables [8]. Moreover, the heat flux profile given by CFD analyses on the "hot part" of the demo has been considered. A scheme of the adopted procedure is reported in the following Figure 17:

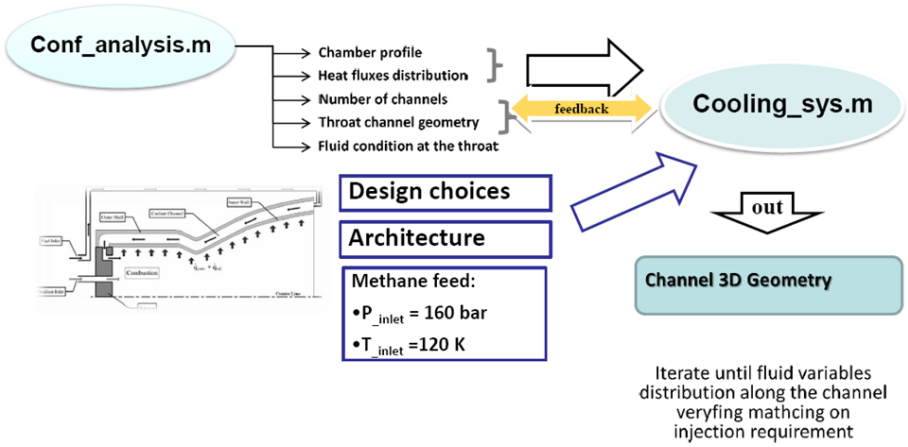

Figure 17: Demo: Scheme of the iterative design procedure [2]

At the end of the procedure, a configuration of cooling channels, characterized by constant parameters (height, width) along the different representative sections (nozzle, throat, convergent, chamber), has been identified. In particular, minimum height values are adopted in the throat section and at the end of the chamber in the downstream direction, as depicted by Figure 18. This strategy has been adopted in order to minimize pressure drops and optimize the thermal efficiency.

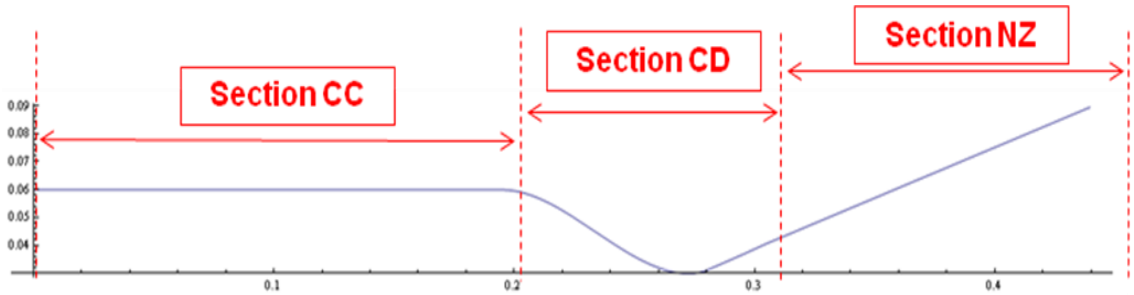

Figure 18: Demo: Key-point sections identified for the design procedure

Thus, a numerical analysis on the demonstrator cooling channel was accomplished by means of ANSYS Fluent v13 [6]. The geometric model and the sketch of the adopted mesh are depicted in Figure 19. The adopted mesh distribution is a structured grid, composed by 25 blocks and 1231000 nodes.

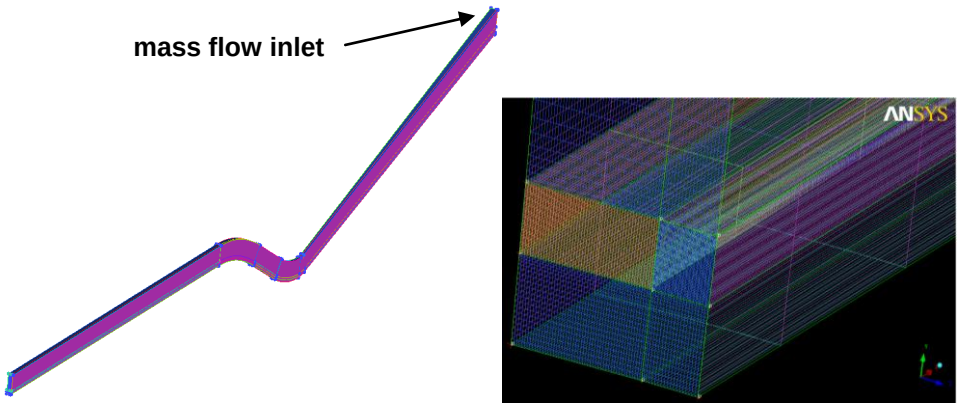

Figure 19: Demo: Regenerative cooling channel

Governing equations of continuity, momentum and energy in the 3-D form were solved under the hypothesis of steady state, NIST real gas model and turbulent flow with thermo-physical properties, evaluated by means of REFPROP v7.0 [8] database, according to the pressure and temperature conditions inside the channel. Also the conduction effects were taken into account because both the liner part and the close-out one were simulated. The channel surfaces were considered rough with a given roughness height, ε. The standard k-ω turbulence model was adopted. A steady-state solution and a pressure based method were chosen to solve the governing equations. A

second-order upwind scheme and the SIMPLE coupling scheme one are chosen for energy and momentum equations and to couple pressure and velocity, respectively [8]. The convergence criteria of 10^{-6} and 10^{-9} for the residuals of the velocity components and energy are assumed, respectively. Simulations were initialized at the inlet section conditions, such as P_{in} = 16.0 MPa and T_{in} = 110 K. The NIST real gas model was activated in the form of single-species flow and also the "liquid" phase was solved if required. In fact, fluid is expected to be in liquid phase at the inlet section and in vapour one from a certain section, according to the applied thermal conditions. The central problem of this analysis consists into simulating the transcritical operating conditions of the working fluid. This behaviour affects also the initialization of the simulation and the convergence history because it is necessary to apply the heat flux by scaling its value and approaching by means of several steps the design value, considering the previous solution as the new starting conditions for the next one, until providing the nominal heat flux, which is depicted by Figure 20.

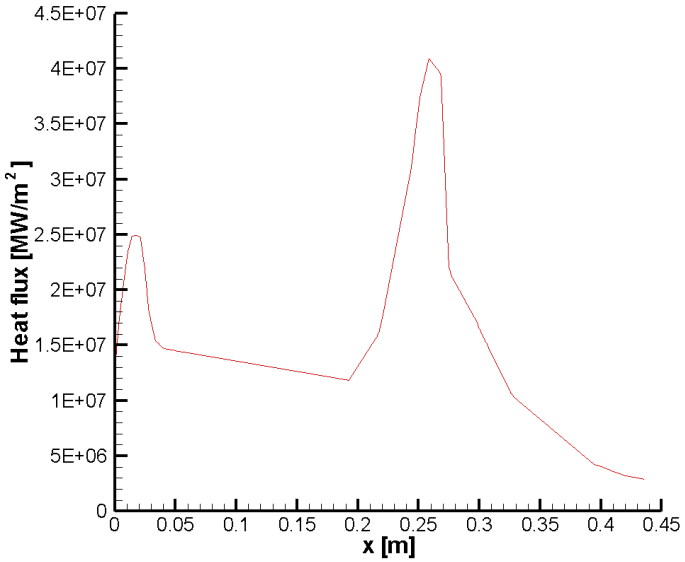

Figure 20: Demo: Heat flux profile applied on the thrust chamber wall

The working fluid was methane, entering the inlet section at T = 110 K and P_{in} = 16.0 MPa while the mass flow rate was set 0.02 kg/s. With reference to Figure 21, the solid material was copper (solid 1), for the liner part, or inconel (solid 2), for the close-out part. Their thermo-physical properties were considered constant with temperature. The upper wall and left outer one were considered adiabatic while the symmetry condition was applied on the right wall. The bottom surface of solid 1 is heated by the heat flux profile, depicted in Figure 20, and it has been applied by means of specific user-defined functions (udf).

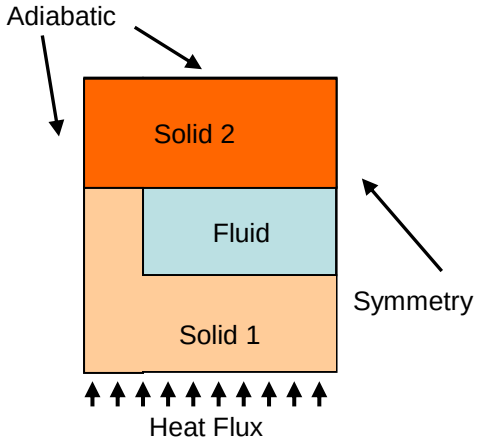

Figure 21: Demo: – Sketch of the model, including materials and boundary conditions

Results show that the throat section, the part most stressed by the thermal power coming from the chamber, is well cooled, and it exhibits temperature values lower than 600 K. However, the fluid properties tend to become deteriorated moving towards the channel outlet section. Thus, in the "chamber section" a large part of the heated wall reaches about 750 K and near the exit section a maximum temperature of about 820 K is detected, as depicted by Figure 22. The mass-weighted temperature at the inlet section is equal to about 425 K. These values of temperature

are associated to the heat flux distribution of Figure 20 coming from a combustion simulation obtained with an imposed temperature at chamber wall of 300 K. A second step of the coupled phenomenon has not yet been done at moment. It should give lower values of heat flux and so lower values of the chamber wall temperature.

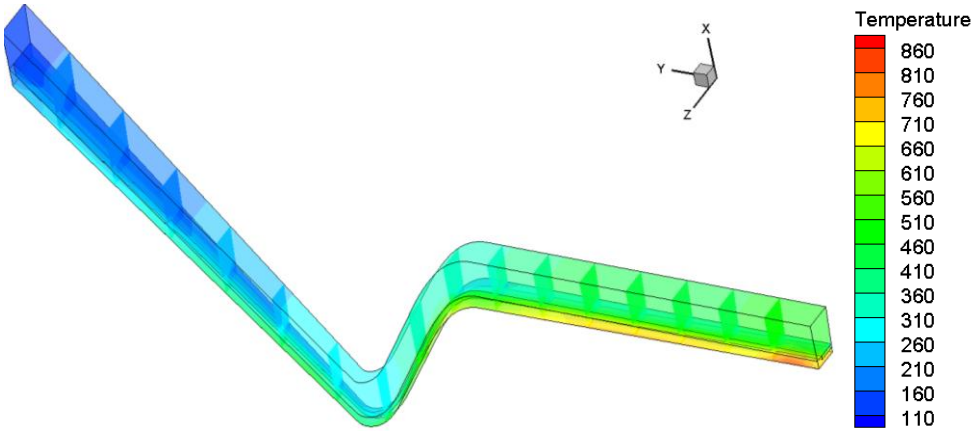

Figure 22: Demo: Temperature distribution on the channel walls and slices along the geometry

Figure 23 reports the results in terms of axial profiles of fluid temperature (a), pressure drops (b), specific heat (c) and thermal conductivity (d), along the cooling channel centre-line plotted on the "symmetry" surface. In particular, a pressure drop of about 4.7 MPa is detected and it is interesting to describe the specific heat profile, which is characterized by a maximum value, detected slightly downstream the throat section while the minimum value of thermal conductivity is detected almost at the beginning of the "chamber section".

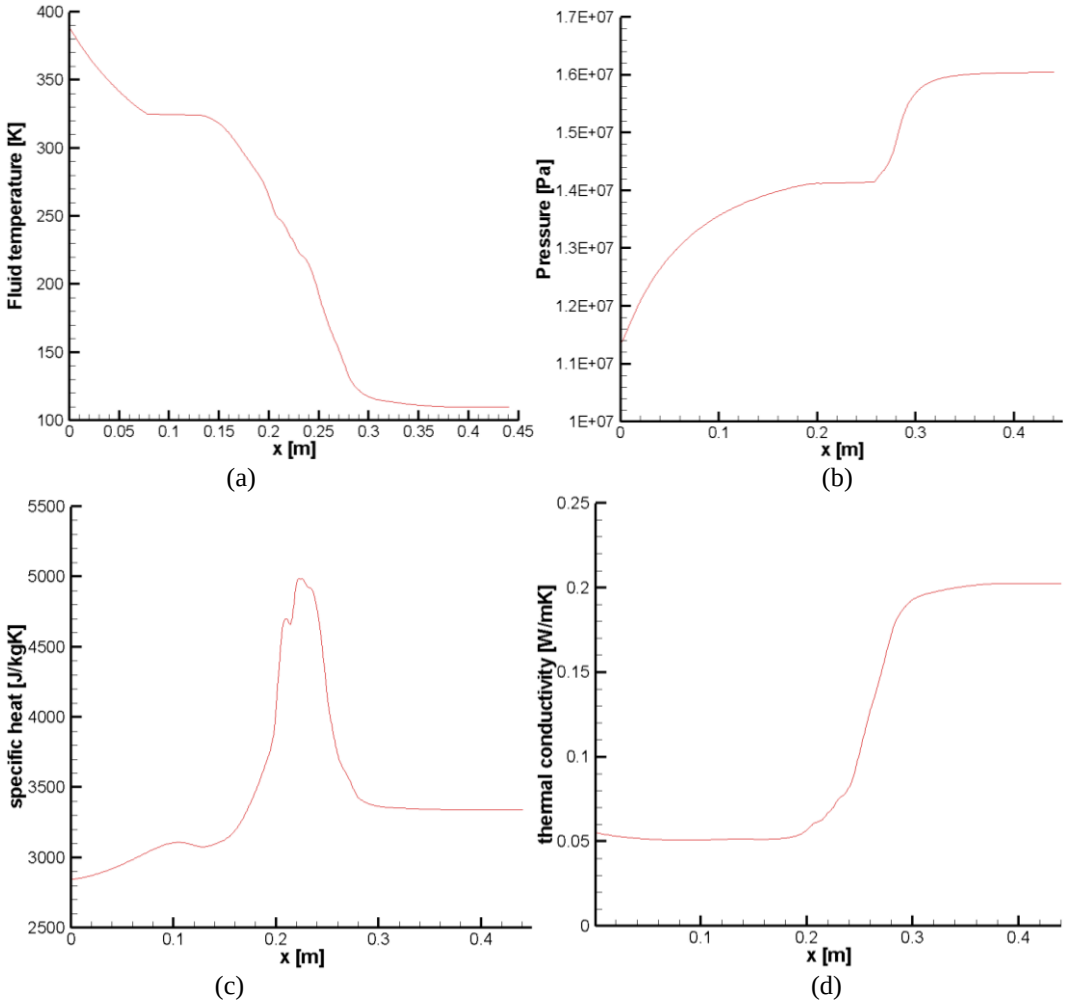

(a) (b)

(c) (d)

Figure 23: Demo 3D cooling channel results

Conclusions

In this work the main results of numerical activities conducted in the framework of the HYPROB BREAD Program have been reported and discussed. The analyses focused on the support to the design process and for this reason the adopted physical modelling is a compromise between accuracy and reasonable convergence CPU time.
It has to be said that one of the aim of the program is also the tuning of numerical tools and strategies that will be validated only after a comparison with the experimental measurements not yet available at moment of writing these notes. Nonetheless the numerical results allowed a deep understanding of basic physical phenomena and gave the input for the thermo-structural analyses and in general useful information for the whole design process.

Acknowledgements

This work has been carried out within the HYPROB program, funded by the Italian Ministry of University and Research (MIUR) whose financial support is much appreciated.

References

[1] Salvatore V., Battista F., Votta R., Di Clemente M., Ferraiuolo M., Roncioni P., Ricci D., Natale P., Panelli M., Cardillo D. and de Matteis P. 2012. Design and Development of a LOX/LCH4 Technology Demonstrator. 48th AIAA/ASME/SAE/ASEE Joint Propulsion Conference & Exhibit, 30 July - 01 August 2012, Atlanta, Georgia.
[2] Battista F., Di Clemente M., Ferraiuolo M., Votta R., Ricci D., Panelli M., Roncioni P., Cardillo D., Natale P. and Salvatore V., 2012. Development of a LOX/LCH4 Technology Demonstrator Based on Regenerative Cooling throughout Validation of Critical Design Aspects with Breadboards in the Framework of the Hyprob Program. 63rd International Astronautical Congress, Naples, Italy. IAC-2012.
[3] Sutton, G.P., Biblarz, O. 2010. Rocket Propulsion Elements. John Wiley & Sons, ISBN-9780470080245.
[4] Pizzarelli M., Nasuti F. and Onofri M. 2008. Flow Analysis of Transcritical Methane in Rectangular Cooling Channels. 44th AIAA/ASME/SAE/ASEE Joint Propulsion Conference & Exhibit 21 - 23 July 2008, Hartford, CT.
[5] ANSYS FLUENT 12.0 Theory Guide 2009, 7.4-7.6. Fluent Inc., Canonsburg, Pennsylvania, USA.
[6] ANSYS FLUENT User's Guide, release 13.0. Ansys Inc., Canonsburg, PA.
[7] ECOSIMPRO, EA Internacional, Magallanes, 3. 28015 Madrid, Spain.
[8] NIST Chemistry WebBook, REFPPROP v7,http://webbook.nist.gov/chemistry/fluid/.
[9] Westbrook C.K. and Dryer F.L. 1981. Simplified Reaction Mechanisms for the Oxidation of Hydrocarbon Fuels in Flames. Combustion Science and Technology , 27, 31-43.
[10] Jones W.P. and Lindstedt R. 1988. Global Reaction Schemes for Hydrocarbon Combustion. Combustion and Flame, 73, 233-249.